

Measurement of P , V , T , and sound velocity across the melting curve of $n\text{-H}_2$ and $n\text{-D}_2$ to 19 kbar

D. H. Liebenberg, R. L. Mills, and J. C. Bronson

Los Alamos Scientific Laboratory, University of California, Los Alamos, New Mexico 87545

(Received 19 June 1978)

We used a piston-cylinder apparatus for simultaneous measurement of P , V , T , and longitudinal sound velocity v_l across the melting line of $n\text{-H}_2$ and $n\text{-D}_2$ at pressures from about 4 to 19 kbar. An equation of the modified Simon type was found to fit the melting-line data satisfactorily. We measured the volume and sound-velocity changes at melting and used these data to infer the Debye temperature, transverse sound velocity, Poisson ratio, compressibility, and entropy in the solid phases. Comparisons with recent theoretical calculations and low-pressure measurements show generally good agreement.

I. INTRODUCTION

At low temperatures or high pressures hydrogen solidifies and at very high pressures it is expected to transform into a metallic state.¹ Many studies of the solid phase have been made in the low-pressure low-temperature region,²⁻⁵ but above about 3 kbar very few measurements are available. Mills and Grilly⁶ measured the melting line at pressures to 3.5 kbar. Along the 4-K isotherm two measurements of pressure-volume dependence were made by Stewart⁷ to 20 kbar and by Anderson and Swenson⁸ to 25 kbar for both hydrogen and deuterium. However, measurements of sound velocity in the solid have been reported³ at pressures up to only 0.2 kbar.

The present study of solid $n\text{-H}_2$ and $n\text{-D}_2$ is part of an ongoing program to investigate the properties of light isotopes of interest to the U. S. Department of Energy. We report measurements of the melting line, change of volume on melting, and longitudinal sound velocity at pressures from 4 to 19 kbar. From these measurements we devise a Simon-type melting curve $P_m(T_m)$, analytically fit the volume change $\Delta V_m(T_m)$, derive a Debye temperature Θ_D using the Lindemann relation, and derive other thermodynamic properties for $n\text{-H}_2$ and $n\text{-D}_2$ solids. Direct comparisons with several theoretical calculations indicate that a finite-temperature model of the solid by Anderson *et al.*⁹ gives sound velocities that reproduce our data quite well. A calculation by Ross¹⁰ is in poor agreement with our measurements of the melting line and our determinations of the Debye temperature, but we show that a downward correction of his pressure can bring agreement. The present measurements of solid hydrogen are the first at pressures greater than 10 kbar along isotherms above 4 K.

II. EXPERIMENTAL

The piston-cylinder apparatus used in these measurements has been described in detail.¹¹⁻¹⁴ Simultaneous measurements are made of volume V and longitudinal sound velocity v_l along isotherms at various temperatures T and pressures P . The unsupported area of a Bridgman seal is used as the mounting surface for a sound transducer that transmits through a buffer-rod plug into the sample where the signal is returned by a fixed-path reflector. For these studies the fixed reflector was designed to be rigid while permitting solid to flow into the measurement region. Either a thin-walled perforated tube or four 0.2-mm-diam pins were used to support the reflector which was scalloped around the rim.

Our procedure for measuring P , V , T , and v_l has been described previously.¹¹⁻¹⁴ In the present study compressions of H_2 and D_2 into the solid region typically took an hour or more to insure that freezing and melting were carried out under equilibrium conditions. The sound velocity and piston displacement were recorded during passage through the two-phase region.

III. RESULTS

As listed in Table I, 19 determinations were made of the melting point and volume change on melting in $n\text{-H}_2$. For most of the points we measured the sound velocity simultaneously, but in some cases distortion of the constant-path reflector or loss of sound signal in the polycrystalline solid prevented measurement of v_l . We accepted solid-phase sound-velocity measurements only when the fluid-phase measurements before and after freezing agreed to within $\pm 0.5\%$.

In $n\text{-D}_2$ some 12 determinations of the melting

TABLE I. Measured values of T_m , P_m , V_s , ΔV_m , and v_l for solid normal hydrogen along the melting curve. Calculated values include the Debye temperature Θ_D , the transverse sound velocity v_t , the adiabatic Poisson ratio σ_s , and the adiabatic compressibility χ_s as discussed in the text.

| T_m (K) | P_m (kbar) | V_s (cm ³ /mole) | ΔV_m (cm ³ /mole) | v_l (km/sec) | Θ_D (K) | v_t (km/sec) | σ_s | χ_s (kbar ⁻¹) |
|--------------|-----------------|----------------------------------|---|-------------------|-------------------|-------------------|------------|-----------------------------------|
| 75.04 | 4.733 | 14.61 | 0.68 | 5.230 | 280 | 2.46 | 0.36 | 0.0376 |
| 75.1 | 4.719 | 14.49 | 0.72 | ... | 281 | ... | ... | ... |
| 75.21 | 4.746 | 14.61 | 0.71 | 5.203 | 280 | 2.46 | 0.36 | 0.0381 |
| 75.21 | 4.763 | 14.63 | 0.69 | 5.12 | 280 | 2.46 | 0.35 | 0.0401 |
| 88.8 | 6.378 | 13.64 | 0.67 | 5.530 | 311 | 2.68 | 0.35 | 0.0322 |
| 89.6 | 6.418 | 13.61 | 0.62 | ... | 313 | ... | ... | ... |
| 100.8 | 7.764 | 13.18 | 0.63 | 5.777 | 336 | 2.87 | 0.34 | 0.0292 |
| 109.2 | 9.010 | 12.81 | 0.52 | ... | 353 | ... | ... | ... |
| 115.5 | 9.779 | 12.53 | 0.50 | 6.334 | 391 | 3.30 | 0.31 | 0.0243 |
| 123.5 | 11.421 | 12.27 | 0.43 | ... | 381 | ... | ... | ... |
| 125.8 | 11.769 | 11.93 | 0.47 | ... | 388 | ... | ... | ... |
| 131.0 | 12.421 | 11.88 | 0.45 | 6.122 | 396 | 3.30 | 0.30 | 0.0256 |
| 133.6 | 12.527 | 11.83 | 0.50 | 6.821 | 400 | 3.28 | 0.35 | 0.0182 |
| 143.7 | 14.852 | 11.35 | 0.44 | ... | 451 | ... | ... | ... |
| 143.8 | 14.626 | 11.38 | 0.43 | 6.908 | 420 | 3.41 | 0.34 | 0.0175 |
| 145.3 | 14.786 | 11.35 | 0.43 | ... | 424 | ... | ... | ... |
| 152.8 | 16.662 | 11.24 | 0.37 | ... | 436 | ... | ... | ... |
| 154.0 | 16.769 | 11.21 | 0.37 | ... | 440 | ... | ... | ... |
| 163.9 | 18.710 | 10.89 | 0.38 | 7.4 | 457 | 3.6 | 0.34 | 0.0146 |

line and volume change on melting were made and are listed in Table II. Simultaneous measurements of v_l were obtained in all but one run. A typical sequence of data along the 95.2-K isotherm is presented in Figs. 1 and 2. Data points for the increasing and decreasing part of the cycle are shown and the corrected pressure is indicated by the dashed curve in Fig. 1. Corrected volumes versus corrected pressures are plotted in Fig. 2 where the melting pressure and the volume change on

melting are indicated by the discontinuity.

The sound-velocity change on melting is shown in Fig. 3 for n -D₂ at $T = 95.2$ K where $P_m = 7.044$ kbar. Measurements in the two-phase region during the freezing process indicated a progressive increase in velocity as the fraction of solid phase increased. A continual loss of signal strength was observed and when solidification was complete a new signal appeared at a higher velocity corresponding to the crystalline phase. As shown

TABLE II. Measured values of T_m , P_m , V_s , ΔV_m , and v_l for solid normal deuterium along the melting curve. Calculated values include the Debye temperature Θ_D , the transverse sound velocity v_t , the adiabatic Poisson ratio σ_s , and the adiabatic compressibility χ_s as discussed in the text.

| T_m (K) | P_m (kbar) | V_s (cm ³ /mole) | ΔV_m (cm ³ /mole) | v_l (km/sec) | Θ_D (K) | v_t (km/sec) | σ_s | χ_s (kbar ⁻¹) |
|--------------|-----------------|----------------------------------|---|-------------------|-------------------|-------------------|------------|-----------------------------------|
| 75.00 | 4.684 | 14.04 | 0.73 | 3.42 | 194 | 1.75 | 0.32 | 0.0505 |
| 75.15 | 4.700 | 13.92 | 0.82 | 3.65 | 194 | 1.74 | 0.35 | 0.0416 |
| 75.19 | 4.700 | 13.99 | 0.82 | 3.73 | 194 | 1.74 | 0.36 | 0.0393 |
| 85.0 | 5.647 | 13.57 | 0.68 | 3.699 | 209 | 1.86 | 0.33 | 0.0409 |
| 94.7 | 7.011 | 12.99 | 0.60 | 3.937 | 224 | 1.96 | 0.33 | 0.0340 |
| 95.1 | 7.044 | 13.09 | 0.57 | 3.930 | 225 | 1.97 | 0.33 | 0.0344 |
| 102.1 | 7.963 | 12.72 | 0.51 | 3.949 | 236 | 2.05 | 0.32 | 0.0341 |
| 115.5 | 10.021 | 12.11 | 0.52 | 4.25 | 254 | 2.18 | 0.32 | 0.0278 |
| 128.4 | 12.109 | 11.64 | 0.45 | 4.193 | 272 | 2.32 | 0.28 | 0.0298 |
| 136.3 | 13.468 | 11.32 | 0.45 | 4.54 | 283 | 2.37 | 0.31 | 0.0231 |
| 145.2 | 14.765 | 11.11 | 0.44 | 5.02 | 294 | 2.42 | 0.35 | 0.0171 |
| 155.7 | 16.967 | 10.76 | 0.39 | ... | ... | ... | ... | ... |

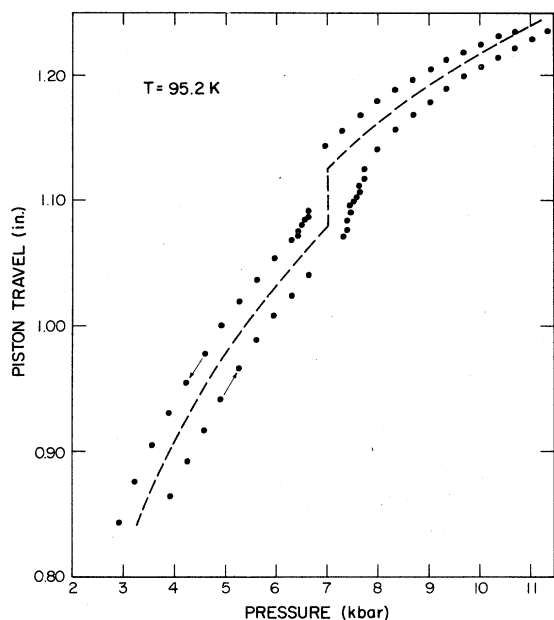


FIG. 1. Measured piston displacement vs pressure in the cell for $n\text{-D}_2$ at $T=95.2$ K. The hysteresis results from internal friction in the movable indium seal at low temperature.

in Fig. 3 measurements at 95.2 K were extended 5 kbar into the solid phase. At other temperatures the measurements were carried less far into the solid phase because lower plasticity limited the flow of solid into the sound cell. In all cases the v_l measurements in solid deuterium were made with a better signal-to-noise ratio than in solid hydrogen.

The melting-curve data were combined with earlier lower-pressure data of Mills and Grilly⁶ and with data obtained near 1 bar by Goodwin¹⁵ for $p\text{-H}_2$. A set of 46 points was used in a least-squares fit to a modified Simon melting equation, resulting in

$$P_m(n\text{-H}_2) = -0.2442 + 2.858 \times 10^{-3} T_m^{1.724} \text{ kbar} \quad (1)$$

where P_m is the melting pressure in kbar and T_m is the melting temperature in Kelvin. A similar fit for $n\text{-D}_2$, using 35 points, gave

$$P_m(n\text{-D}_2) = -0.5431 + 3.666 \times 10^{-3} T_m^{1.677} \text{ kbar}. \quad (2)$$

In the case of $n\text{-D}_2$ only the earlier data of Mills and Grilly⁶ were used to augment our measurements. The accuracy of the measured points is similar to that discussed in Refs. 13 and 14. The fit of data to Eqs. (1) and (2) was such that the variance is 0.013 for $n\text{-H}_2$ and 0.0035 for $n\text{-D}_2$.

Since the volume change on melting is typically only about 4% of the fluid volume, the uncertainty in the present determination of ΔV_m is rather high, about 10%–15%. A least-squares fit was made to

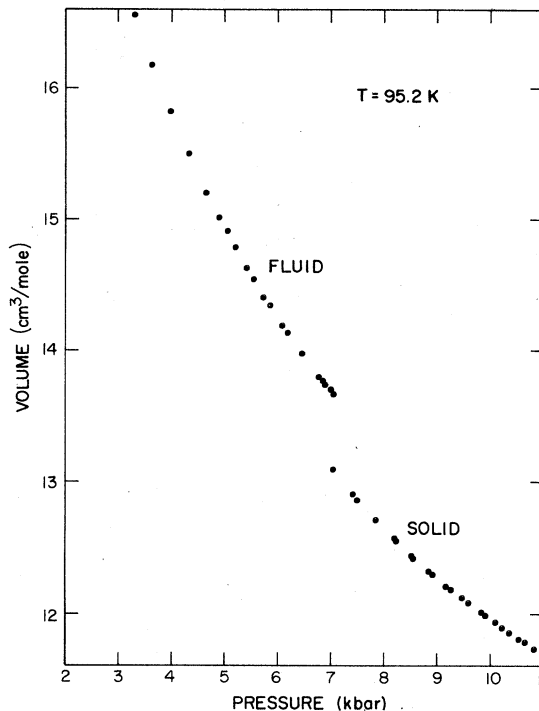


FIG. 2. Sample volume vs pressure for $n\text{-D}_2$ at $T=95.2$ K. The volume change on melting is represented by the discontinuity.

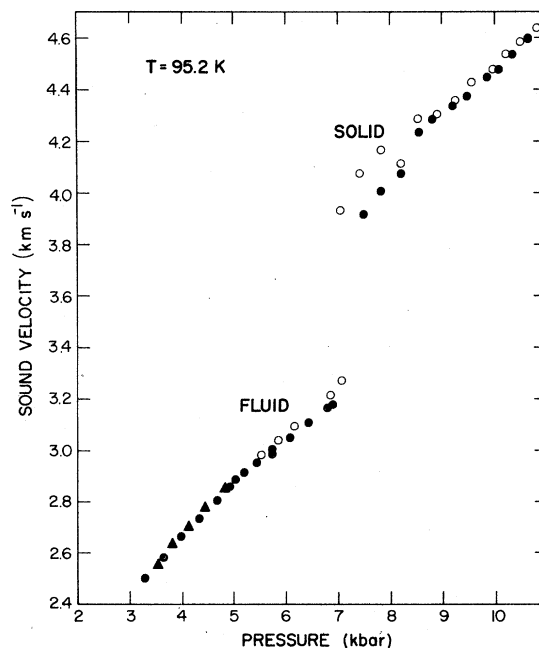


FIG. 3. Sound velocity vs pressure across the melting line for $n\text{-D}_2$ at $T=95.2$ K. The gradual increase in velocity through the two-phase region during melting is not shown. Closed and open circles represent measurements during the increasing and decreasing pressure cycle, respectively. Triangles are from a second increase in pressure.

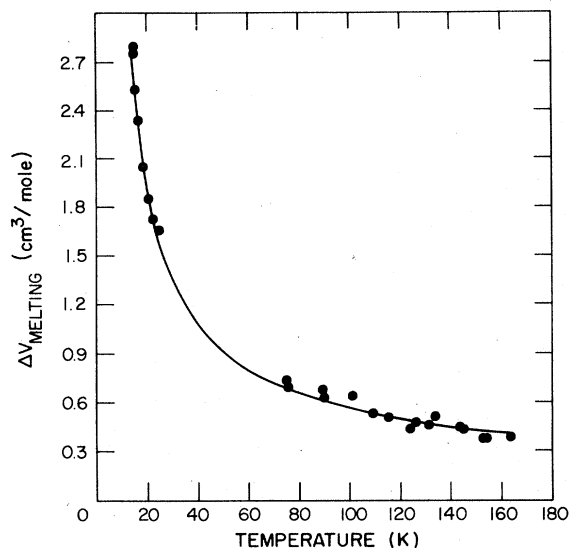


FIG. 4. Volume change on melting vs temperature for n -H₂. The low-temperature points were obtained from Ref. 6 and the present points were taken at $T > 75$ K. The smooth curve is a least-squares fit to Eq. (3).

the 27 data points for n -H₂ including the earlier low-pressure data of Mills and Grilly,⁶ and the resultant power law was

$$\Delta V_m(n\text{-H}_2) = 9.355(T_m - 6.720)^{-0.6200} \text{ cm}^3/\text{mole}. \quad (3)$$

A similar fit to the 23 points for deuterium gave

$$\Delta V_m(n\text{-D}_2) = 38.49(T_m + 0.1265)^{-0.9093} \text{ cm}^3/\text{mole}. \quad (4)$$

Measured values are presented in Tables I and II and are plotted for n -H₂ in Fig. 4 along with Eq. (3).

IV. DISCUSSION

A. Melting line

A Simon-type function¹⁶ was used to describe the hydrogen and deuterium melting lines in Eqs. (1) and (2). Near the triple point these equations give large errors and the compilation of Roder *et al.*¹⁷ should be consulted. From 1 to 18 kbar our standard deviation and percentage error in P_m for n -H₂ are 0.11 kbar and 1.4%, respectively, and for n -D₂ they are 0.08 kbar and 1.0%.

Recently Kechin *et al.*¹⁸ measured the melting line in hydrogen to 10 kbar. Their values and our Eq. (1) have a standard deviation of 0.34 kbar. However when their relatively large error of 1 K in temperature is considered the disagreement drops to 0.24 kbar. Since they rely on the fluid equation-of-state (EOS) data of Tsiklis *et al.*¹⁹ whose measurements at pressures up to 7 kbar are in good agreement with ours,¹⁴ the discrepancy is hard to explain. Comparison of their molar volumes in the solid with our EOS in Ref. 14 and Eq. (3) gives a standard deviation of 0.28 cm³/mole,

which is nearly within the combined estimated errors of ± 0.20 cm³/mole in their work and ± 0.06 cm³/mole in ours.

Ross¹⁰ obtained theoretical values of the melting line at pressures and temperatures greater than the present measurements. Since the earlier melting line of Mills and Grilly⁶ could be extrapolated by a factor of 5 in pressure with only a 1% error, we felt justified in extrapolating Eq. (1) by a factor of two in P_m for comparison with Ross¹⁰ in the range $250 < T_m < 300$ K. At the lowest temperature we find $P_m = 38.6$ kbar compared to the Ross value $P_m = 78$ kbar. This discrepancy is far outside the range of experimental error.

Another calculation of the melting line for hydrogen was made by Grigorev *et al.*²⁰ Over our experimental range $75 < T_m < 165$ K their equation predicts a larger melting pressure for a given temperature. At $T_m = 165$ K the predicted melting pressure is 19.9 kbar or 6% too large while at $T_m = 250$ K the predicted value is 7% above Eq. (1), but much closer to our value than to that of Ross.¹⁰

B. Molar volume

In earlier papers^{14,21} we reported simultaneous measurements of v_l and V_f for fluid n -H₂ and n -D₂ in the $75 < T < 300$ K and $2 < P < 20$ kbar range. These data were fitted to an EOS that gave calculated molar volumes in disagreement by only $\pm 0.4\%$ with measured values. By combining the results from this EOS at the melting curve with the measured ΔV_m , the molar volume of the solid V_s can be obtained. These results when plotted on a $\ln V_s$ - T surface as isobars should extrapolate to the low-temperature values of Stewart⁷ and Anderson and Swenson⁸ at 4.2 K. The slope $(\partial \ln V_s / \partial T)_p \rightarrow 0$ at $T = 0$ K and graphical curves satisfying these constraints fit the data with an estimated error of $\pm 0.5\%$. We measured molar volumes well into the solid phase at several temperatures. Along the 75-K isotherm where $P_m = 4.7$ kbar the measurements extended to 11 kbar. Our accuracy in the solid region depends on whether solid hydrogen flows plastically in the chamber. The generally good fit by extrapolation to the 4-K isotherm data^{7,8} suggests that nonhydrostatic effects are small.

The quantity ΔV_m decreases with increasing temperature as shown in Eq. (3) and Fig. 4. Even at the calculated¹⁰ pressure of 2.5 Mbar for the transition from a molecular to a metallic phase our molar volume change is finite and has the extrapolated value $\Delta V_m = 0.07$ cm³/mole. By comparison, the equation suggested by Kechin *et al.*¹⁸ extrapolates to a zero volume change at 526 kbar, well below the expected molecular-metal phase transition.

C. Ultrasonic velocity

The present ultrasonic longitudinal velocities in solid hydrogen and deuterium as illustrated in Fig. 3 are the only ones available in this pressure region. Difficulties with solid formation in the fixed-path sound cage limited the accuracy of our results to $\pm 3\%$ except at the lowest temperature in deuterium where the error was somewhat larger. Values of the sound velocity for $n\text{-H}_2$ and $n\text{-D}_2$ may be compared in Tables I and II. Kinetic theory suggests that $v_l(\text{H}_2)/v_l(\text{D}_2) = (M_{\text{D}_2}/M_{\text{H}_2})^{1/2}$, where M_{D_2} and M_{H_2} are the molecular weights of deuterium and hydrogen, respectively. This relation is approximately obeyed, as we found in the high-pressure fluid,²¹ and is in contrast to measurements in the low-pressure solid³ where the ratio is much closer to one. However, as may be seen in the data of Ref. 3 for pressures at 0.3 kbar, the velocities are diverging so that a smooth extrapolation to the present result is possible.

D. Debye temperature

The Debye temperature for the solid phase along the melting line can be calculated from the Lindemann²² melting equation,

$$C^2 = \Theta_D^2 V_s^{2/3} M / T_m, \quad (5)$$

where C is a constant that we assume has the same value as for nitrogen,¹³ namely $C = 116 \pm 2 \text{ cm K}^{1/2} \text{ g}^{1/2} \text{ mole}^{-5/6}$. This compares to a value of $C = 114$ obtained by Domb²³ for low-pressure hydrogen. The calculated values of Θ_D along the melting line for $n\text{-H}_2$ are shown in Fig. 5. Low-pressure values were taken from a tabulation by Goldman²⁴ and Ahlers.²⁵ The Debye temperature that we calculate from the work of Kechin *et al.*¹⁸ using Eq. (5) is in good agreement up to their maximum pressure of 9.8 kbar. Geilikman and Ivanter²⁶ calculated the pressure dependence of Θ_D at zero temperature in the solid. At all pressures their calculated values are within 2% of ours.

Ross¹⁰ has calculated values of Θ_D from a theoretical model for solid hydrogen. As already discussed there is poor agreement between his values extrapolated to lower pressures and ours obtained from Eq. (5) using our melting curve. However, if we use our melting-curve data to correct the melting pressures given by Ross¹⁰ the values of Θ_D along the revised melting line shown in Fig. 5 are in good agreement with a smooth extrapolation of our data. Although not included in Fig. 5 the values of Geilikman and Ivanter²⁶ are within 5% of the revised Ross values in the region of overlap.

Similar calculations of the Debye temperature in $n\text{-D}_2$ are shown in Table II. At low pressures the values are identical to those for hydrogen, but at 0.2 kbar, the maximum pressure obtained by

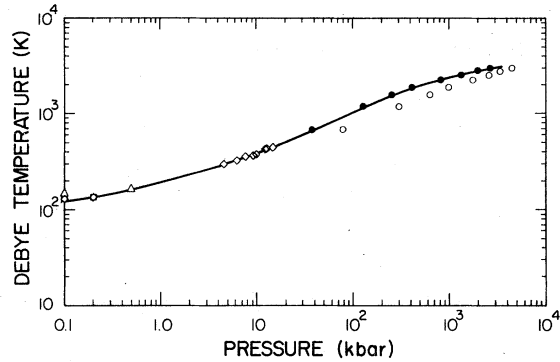


FIG. 5. Debye temperature vs pressure for $n\text{-H}_2$ along the melting line. \square , Brickwedde *et al.* as cited in Ref. 24; \triangle , Ahlers, Ref. 25; \diamond , present results; \circ , Ross, Ref. 10; \bullet , Ross corrected values discussed in text. The smooth line is a visual aid.

Wanner and Meyer,³ the Debye temperature for hydrogen rises above that for deuterium. This trend continues to the higher pressures of the present measurements.

E. Transverse sound velocity, compressibility, and Poisson's ratio

From the Lindemann relation for Θ_D , coupled with the measured longitudinal sound velocity, and the assumption of an isotropic crystal we estimated the transverse sound velocity in $n\text{-H}_2$ and $n\text{-D}_2$ according to the following relation which we used earlier¹³ for solid nitrogen

$$\Theta_D = \frac{\hbar}{k} \left(\frac{6\pi^2 N}{V_s} \right)^{1/3} \left[\frac{1}{3} \left(\frac{1}{v_l^3} + \frac{2}{v_t^3} \right) \right]^{-1/3}, \quad (6)$$

where \hbar , k , N have their usual notation and v_l and v_t are the ultrasonic longitudinal and transverse velocities, respectively, averaged over a polycrystalline symmetric solid. Computations along the melting line are listed in Tables I and II. No other values have been reported for either v_l or v_t in this pressure region. However in Fig. 6 we compare our measurements of v_l and our derived v_t at melting with those calculated by Anderson *et al.*⁹ using a finite-temperature theory. There is excellent agreement between experiment and theory.

Using similar approximations¹³ for the polycrystalline sample we estimated the adiabatic compressibility of the solid and the adiabatic Poisson ratio from

$$\chi_s = V_s [M(v_l^2 - \frac{4}{3}v_t^2)]^{-1}, \quad (7)$$

and

$$\sigma_s = \frac{1}{2} [(v_l/v_t)^2 - 2][(v_l/v_t)^2 - 1]^{-1}. \quad (8)$$

Calculations of χ_s and σ_s along the melting line are given in Tables I and II. The adiabatic compressibilities of solid $n\text{-H}_2$ and $n\text{-D}_2$ are the

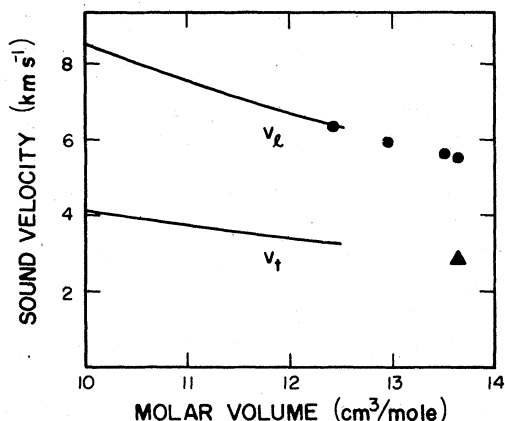


FIG. 6. Longitudinal and transverse sound velocity in solid n -H₂ at 91 K. ●, present measurement for v_l ; ▲, calculated value for v_t as discussed in text; smooth curve, calculation by Anderson *et al.*, Ref. 9.

same within the error of calculation. At 4 K and 15 kbar the isothermal compressibility determined by Anderson and Swenson⁸ is 0.016 kbar⁻¹ for n -H₂ and 0.015 kbar⁻¹ for n -D₂. As one might expect the solid phase is stiffer at low temperatures for a given pressure.

Calculations giving ~ 0.3 for the Poisson ratio of solid n -H₂ at high pressures are consistent with low-pressure computations.^{3,27} Thus for solid n -H₂ there is satisfactory agreement among various sets of data at low pressure and the present high-pressure measurements, even though several simplifying assumptions have been made. The Poisson ratio for solid n -D₂ is not significantly larger than for n -H₂ within the estimated $\pm 10\%$ error of calculation.

F. Entropy change

We computed the entropy change on melting, ΔS_m , from the Clapeyron relation using for n -H₂ Eqs. (1) and (3) and for n -D₂ Eqs. (2) and (4). The result for hydrogen with T_m in Kelvin is

$$\Delta S_m/R = 0.554T_m^{0.724}(T_m - 6.72)^{-0.620}. \quad (9)$$

The melting entropy computed from Eq. (9) exhibits a minimum at $T_m = 46.7$ K ($P_m = 1.9$ kbar) as shown in Fig. 7. At the triple point temperature of 13.95 K, which is well below our range of measurements, Eq. (9) gives $\Delta S_m/R = 1.09$ compared to a literature value¹⁷ of 1.01. The entropy of melting is relatively small because hydrogen, unlike many substances, shows little change in rotational energy across the transition and, indeed, hydrogen molecules rotate freely in the solid down to zero Kelvin.

At melting temperatures above 300 K Eq. (9) can be approximated by $\Delta S_m/R \cong 0.554T_m^{0.1}$ with an er-

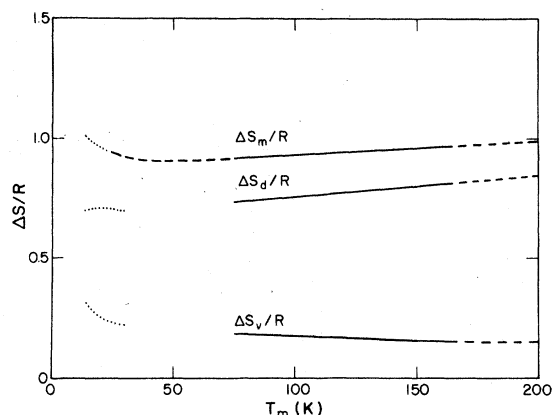


FIG. 7. Entropy contributions to total melting entropy $\Delta S_m/R$ of n -H₂ due to change in volume $\Delta S_v/R$ and molecular disorder $\Delta S_d/R = \Delta S_m/R - \Delta S_v/R$. Solid line, calculated from Eqs. (9)–(11) as discussed in text; dashed line, extrapolation of Eqs. (9)–(11); dotted line, calculated from Refs. 17 and 28.

ror of less than 3%. In this region the entropy difference between fluid and solid increases with T_m (or P_m), contrary to our earlier observation¹³ for N₂.

It is possible to compute absolute entropies in solid H₂ at fusion by extending our previous fluid entropies¹⁴ to the melting curve using Eq. (1) and applying Eq. (9). Similar calculations can be made for n -D₂.²¹

Along the melting curve at low temperatures, fluid n -H₂ is in equilibrium with disordered hexagonal solid. However, there is recent evidence²⁹ that above $T_m \cong 15$ K the fluid region is bounded by an fcc phase. In an attempt to learn more about the solid-fluid transition in H₂ we carried out an analysis similar to the one we described¹³ for N₂ in which the melting entropy was broken down into two terms,

$$\Delta S_m = \Delta S_v + \Delta S_d, \quad (10)$$

where ΔS_v is the entropy change due solely to the volume expansion and ΔS_d is the residual entropy change due to disordering of the molecules. The term ΔS_v can be calculated following Turturro and Bianchi³⁰ from the relation

$$\Delta S_v = \int_{V_s}^{V_f} \left(\frac{\partial P}{\partial T} \right)_v^{T_m} dV, \quad (11)$$

in which $(\partial P/\partial T)_v^{T_m}$ is the isochoric pressure coefficient, evaluated at T_m , and is integrated over the solid-fluid volume change at melting, $\Delta V_m = V_f - V_s$. Equations (1) and (3) were used in conjunction with Eq. (11) from Ref. 14 to calculate ΔS_v and the results along with ΔS_d from Eq. (10) are plotted as dimensionless quantities in Fig. 7. Figure 7 shows that there are gaps in the calcula-

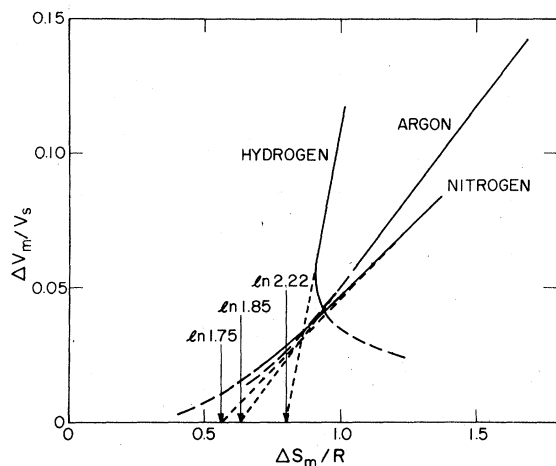


FIG. 8. Relative volume change vs entropy change on melting. Argon and nitrogen, Ref. 13; solid line, experimental range; dashed line, extrapolated melting equations; dotted line, extension of initial slope to intercept (arrow).

tions over the interval $30 < T_m < 75$ K, but apparently the curves can be joined smoothly. The entropy of disorder, $\Delta S_d/R$ rises from about $\ln 2.0$ near the triple point to about $\ln 2.2$ at our highest melting temperature. In the case¹³ of N_2 and Ar

this quantity exhibited constant values of $\ln 1.75$ and $\ln 1.85$, respectively, all along the melting curves.

Stishov *et al.*³¹ attempted to extract the entropy of disorder on melting by plotting $\Delta S_m/R$ vs $\Delta V_m/V_s$ for argon and sodium and found that as $\Delta V_m/V_s \rightarrow 0$, $\Delta S_m/R \rightarrow \ln 2.0$. We present a similar plot for $n\text{-H}_2$ in Fig. 8 where comparison is made with our earlier¹³ curves for Ar and N_2 . Starting at the triple point the hydrogen data at low T_m fall on a linear curve that extrapolates to $\ln 2.22$ as $\Delta V_m/V_s$ goes to zero. The behavior is clearly different at high temperatures, however, where $\Delta S_m/R$ rises with increasing T_m , resulting in a negative slope. Although not shown in Fig. 8, curves for ^3He and ^4He exhibit negative slopes over the entire experimental region.³² At present we are unable to attach any significance to plots such as those in Fig. 8.

ACKNOWLEDGMENTS

We thank L. C. Schmidt for constructing and assembling the piston-cylinder apparatus. The work was performed under the auspices of the U. S. Department of Energy and was supported in part by the Materials Science Section of the Division of Physical Research.

¹E. Wigner and H. B. Huntington, *J. Chem. Phys.* **3**, 764 (1935); other references, in Jean-Léon Masse, *Equation d'Etat de L'Hydrogene Solide a O °K*, Report No. CEA-BIB-220, 1976 (unpublished).

²P. A. Bezuglyi, R. O. Plakhotin, L. M. Taresenko, *Sov. Phys. Solid State* **13**, 250 (1971).

³R. Wanner and H. Meyer, *Phys. Lett. A* **41**, 189 (1972); *J. Low Temp. Phys.* **11**, 715 (1973).

⁴J. P. McTague, in *Lattice Dynamics and Intermolecular Forces*, edited by S. Califano (Academic, New York, 1975), pp. 302-313.

⁵I. F. Silvera, in Ref. 4, pp. 277-301.

⁶R. L. Mills and E. R. Grilly, *Phys. Rev.* **101**, 1246 (1956).

⁷J. W. Stewart, *J. Phys. Chem. Solids* **1**, 146 (1950).

⁸M. S. Anderson and C. A. Swenson, *Phys. Rev. B* **10**, 5184 (1974).

⁹A. B. Anderson, J. C. Raich, and L. B. Kanney, *Phys. Rev. B* **15**, 5804 (1977).

¹⁰M. Ross, *J. Chem. Phys.* **60**, 3634 (1974).

¹¹D. H. Liebenberg, R. L. Mills, and J. C. Bronson, *J. Appl. Phys.* **45**, 741 (1974).

¹²R. L. Mills, D. H. Liebenberg, and J. C. Bronson, *J. Chem. Phys.* **63**, 1199 (1975).

¹³R. L. Mills, D. H. Liebenberg, and J. C. Bronson, *J. Chem. Phys.* **63**, 4026 (1975).

¹⁴R. L. Mills, D. H. Liebenberg, J. C. Bronson, and L. C. Schmidt, *J. Chem. Phys.* **66**, 3076 (1977).

¹⁵R. D. Goodwin, *Cryogenics* **2**, 353 (1962).

¹⁶F. E. Simon, *Z. Elektrochem.* **35**, 618 (1929); *Trans. Faraday Soc.* **33**, 65 (1937); *Proc. R. Soc. A* **218**, 291 (1953).

¹⁷H. M. Roder, G. E. Childs, R. D. McCarty, and P. E. Angerhofer, *Natl. Bur. Stand. (U.S.) Tech. Note* 641, 1973 (unpublished).

¹⁸V. V. Kechin, A. I. Likhter, Yu. M. Pavlyuchenko, L. Z. Ponzovsky, and A. N. Utuzh, *Zh. Eksp. Teor. Fiz.* **72**, 345 (1977) [*Sov. Phys. JETP* **45**, 182 (1977)].

¹⁹D. S. Tsiklis, V. Ya. Maslennikova, S. D. Gavrilov, A. N. Egorov, and G. V. Timofeeva, *Dok. Akad. Nauk (USSR)* **220**, 1384 (1975).

²⁰F. V. Grigorev, S. B. Kormer, O. L. Mikhailova, A. P. Tolochko, and V. D. Urlin, *Zh. Eksp. Teor. Fiz.* **69**, 743 (1975) [*Sov. Phys. JETP* **42**, 378 (1976)].

²¹R. L. Mills, D. H. Liebenberg, and J. C. Bronson, *J. Chem. Phys.* **68**, 2663 (1978).

²²F. A. Lindemann, *Z. Phys.* **11**, 609 (1910).

²³C. Domb, *Nuovo Cimento Suppl.* **9**, 9 (1958).

²⁴V. V. Goldman, *J. Low Temp. Phys.* **24**, 297 (1976).

²⁵G. Ahlers, *J. Chem. Phys.* **41**, 86 (1964).

²⁶B. T. Geilikman and I. G. Ivanter, *Fiz. Nizk. Temp.* **2**, 768 (1976) [*Sov. J. Low Temp. Phys.* **2**, 378 (1976)].

²⁷P. A. Bezuglyi, R. O. Plakhotin, and L. M. Tarasenko, *Sov. Phys. Solid State* **13**, 250 (1971).

²⁸R. D. McCarty, *Natl. Bur. Stand. (U.S.) Tech. Note* 617, 1972 (unpublished).

²⁹R. L. Mills, *J. Low Temp. Phys.* **31**, 423 (1978).

³⁰A. Turturro and U. Bianchi, *J. Chem. Phys.* **62**, 1668 (1975).

³¹S. M. Stishov, I. N. Makarenko, V. A. Ivanov, and A. M. Nikolaenko, *Phys. Lett. A* **45**, 18 (1973).

³²E. R. Grilly and R. L. Mills, *Ann. Phys. (N.Y.)* **8**, 1 (1959).